Observation of an interplay between single-electron charging effects and superconductivity in YNi_2B_2C

Eyal Bar-Sadeh and Oded Millo*
Racah Institute of Physics, The Hebrew University, Jerusalem 91904, Israel
(Received 31 July 1995; revised manuscript received 5 September 1995)

Cryogenic scanning tunneling microscopy is employed in studies of YNi_2B_2C in the superconducting phase. Samples prepared with Ni deficiency exhibit a sharp superconducting transition, onset around 15 K, while the local scanning tunneling spectroscopy measurements reveal granular properties. We have also measured I-V characteristics that manifest an interplay between single electron charging effects and superconductivity. Some of these characteristics show features consistent with tunneling into a small superconducting particle. Others correspond to tunneling into isolated metallic particles weakly coupled to a superconducting environment.

The interplay between charging effects and superconductivity plays a dominant role in the conductance properties of granular superconductors. In such systems there are two important energy scales. One is the charging energy due to single electron tunneling onto a grain, $E_c=e^2/2C$, where C is the grain capacitance with respect to its environment, and the other is the superconductor energy gap, 2Δ (and consequently the Josephson coupling energy). In order to experimentally observe an interplay between charging effects and superconductivity these two energies must be of the same order of magnitude. The interest in this subject has not decayed since the early studies of disordered granular superconductors.[1] Today, much experimental effort is focused on nanofabricated ordered arrays of Josephson tunnel junctions[2] and superconducting double-barrier tunnel junctions (DBTJ).[3,4] The *normal* DBTJ configuration, where a small metallic grain is coupled via two tunnel junctions to metallic macroscopic electrodes, has been widely studied in connection with single electron charging (SEC) effects such as the Coulomb blockade and the Coulomb staircase.[5–7] If the capacitance of the island with respect to its environment is small enough, so that E_c exceeds the thermal energy k_BT, Coulomb blockade can be observed experimentally. The width of the Coulomb blockade (the region where the tunneling current is suppressed) depends on the effective fractional residual charge,[5–7] Q_0, on the central electrode. When $Q_0=0$ the width is maximal, whereas for $Q_0=\pm e/2$ the Coulomb blockade is completely suppressed. For asymmetric DBTJ a Coulomb staircase is observed, consisting of a series of equidistantly spaced steps in the I-V traces. In the case where one or more of the electrodes is a superconductor, additional features can be clearly observed in the I-V characteristics due to an interplay between SEC effects and superconductivity.[3,4] The signature of this interplay is evident also in disordered granular superconductors, especially in the vicinity of the superconductor-to-insulator transition.[8] These systems, and disordered granular systems in general, have been studied so far mainly on macroscopic scales, therefore losing important information on the spatial fluctuations of the local conductance that may be very prominent.[9] The advent of scanning tunneling microscopy (STM) now provides the tool to measure electronic and transport properties *locally*, as was demonstrated in studies of granular metals[9] and superconductors.[10,11]

In this paper we present a cryogenic STM study of granular YNi_2B_2C samples which exhibit *global* superconductivity but contain about 20% of a nonsuperconducting impurity phase. Our spatially resolved tunneling-spectroscopic data show rapid and sharp transitions from fully superconducting to fully normal regions.[10] These data can be attributed to a granular normal-superconductor material with weak coupling, i.e., large contact resistance, between neighboring grains. In addition, our tunneling I-V characteristics often manifest SEC effects, frequently in conjunction with superconductivity. These charging effects are usually observed when the STM tip is situated above a nanometer-scale surface grain, which is probably weakly coupled to its environment (large neighboring grains). Some of the features we observe in these characteristics are similar to those reported[3,4] for nanofabricated DBTJ containing superconducting electrodes. However, other features are also revealed in our STM experiments, mainly due to the fact that we can easily and continuously change the degree of asymmetry of our DBTJ configurations as well as the value of Q_0. Such changes are achieved simply by varying the tip-grain separation,[6,7,9–11] as will be discussed below. Our results are consistent with those of McGreere *et al.*,[11] that were obtained for Pb films. However, the I-V curves presented by these authors correspond *only* to the all-superconductor DBTJ configuration. In our experiment other DBTJ configurations have been realized due to the granular normal-superconductor nature of our samples.

In order to ensure the significant presence of a nonsuperconducting phase we have prepared the samples by melting *nonstoichiometric* elemental constituents, with some Ni deficiency. A relatively sharp superconducting transition was observed[10] at $\sim$15.0 K, somewhat lower than the transition temperature measured for pure samples,[12] $T_c=15.6$ K. The x-ray-diffraction pattern indicates that the major phase ($\sim$80%) consists of a body-centered tetragonal structure with lattice parameters corresponding to YNi_2B_2C in the superconducting phase.[12] The pattern contains several impurity peaks corresponding to YB_2C_2 ($\sim$20%) and some other unidentified extra lines (less than 3%). Specimens were sliced from the ingot and then polished, first by fine Al_2O_3 powder

and ending with 0.25 μm diamond lapping compound, just before mounting in our homemade cryogenic STM. The STM was immersed in liquid He right after evacuating the sample space, and the sample and the scanhead were cooled down to 4.2 K via He exchange gas. The STM topographic images were measured in the constant current mode, where a feedback circuit controls the tip-sample separation for a given setting of the tunneling current, I_s, and tip bias, V_s. The I-V curves, on the other hand, were acquired while momentarily disconnecting the feedback circuit.

A signature of granularity in these samples is the rapid spatial transition from superconducting to normal behavior, as demonstrated by Fig. 3 of our previous publication, Ref. 10. There we report on reproducible rapid spatial transitions from superconducting to normal regions on length scales of $\sim$20 nm. The superconducting gap parameter, Δ, was determined from fitting the finite-temperature BCS theory for normal-insulator-superconductor (NIS) tunnel junctions[13] to I-V characteristics that were taken at *large* superconducting regions, and it was found to have the value of 2.55 ± 0.05 meV. We wish to point out that in these large spatial regions the width of the apparent gap in the I-V curves was insensitive to changing the STM setting for a wide range of tunneling resistances. Thus the gap observed in these regions cannot be even partly associated with SEC effects. (It will be shown below that charging acts to increase the apparent gap in the I-V traces.) We may therefore conclude that region (a) in Fig. 3 of Ref. 10 is a very large grain, strongly coupled to the ''infinite'' superconducting cluster (recall that our samples show global superconductivity), and thus $\Delta\cong2.55$ meV indeed represents the gap parameter of the *bulk* superconductor. The spatial transition from superconducting to normal regions have *always* occurred across grain boundaries which were clearly observed in the topographic images. This suggests that our samples consist of randomly dispersed and, in many cases, weakly-coupled superconducting and normal grains, and thus may be described as a granular normal-superconductor system. Evidence for this picture serves the observation that I-V characteristics that were taken on apparently *small* grains ($\sim$10 nm in diameter) often depicted SEC effects, frequently in parallel with superconductivity.

In Ref. 10 we have presented I-V characteristics measured on YNi_2B_2C which conform to the all-normal DBTJ configuration. These data were quantitatively accounted for assuming a small metallic (normal) surface grain weakly coupled to the STM tip and to large normal neighboring grains. There are, however, other possible DBTJ configurations that can be realized in our experiment, where the STM tip was made of a normal metal (Pt-Ir). One is when the grain is superconducting but the surrounding substrate is normal, to be referred to as the NISIN configuration. Another configuration is a normal grain weakly coupled to a superconducting environment (NINIS configuration). Finally, it is possible that both the small grain and its surroundings are superconducting (NISIS configuration). These three configurations may yield an interesting interplay between SEC effects and superconductivity, as will be discussed in the rest of the paper.

In Fig. 1 we present two experimental I-V traces (displaced for clarity) that were measured at the *same* lateral position, on a surface grain $\sim$8 nm in diameter, but with *different* STM settings. Both were measured with the same V_s but with a slightly different I_s, yielding a significant change in Q_0 (but not in the tip-sample separation; see below). While the experimental curve (b) displays a gap structure typical to the Coulomb blockade in DBTJ, curve (a) displays a superconductor-gap structure typical for NIS tunnel junctions. These data can be accounted for by the NINIS configuration. When $Q_0=e/2$ the Coulomb blockade is completely suppressed, the grain is effectively ''transparent'' even at small bias voltages, and thus the quasiparticle density of states (DOS) of the superconducting environment is reflected in the I-V trace. On the other hand, when $Q_0=0$ the Coulomb blockade is fully developed, and if $E_c\geqslant\Delta$ the gap opened in the tunneling DOS due to grain charging masks the superconductor DOS of the substrate. [A more complex behavior is found for other values of Q_0; this is shown in Fig. 3(b).] The smooth lines in the figure represent theoretical calculations based on the assumed NINIS tunneling configuration. (Each theoretical curve was displaced for clarity from the corresponding experimental trace.) Curve (b) was calculated from the ''orthodox'' model[5,6] of the DBTJ configuration with $Q_0=0$ and capacitances $C_1=2.0\times10^{-17}$ F and $C_2=0.55\times10^{-17}$ F, for the tip-grain and grain-bulk junctions, respectively. Curve (a) was calculated from the BCS theory for NIS tunnel junction with $\Delta=2.55$ meV. The two theoretical curves are seen to fit very well to the experimental curves.

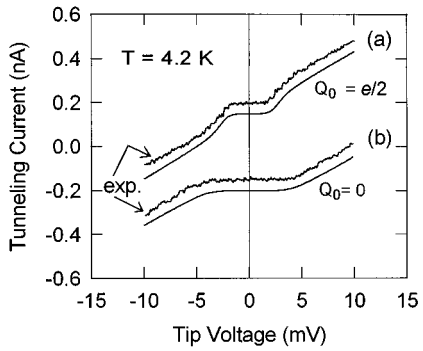

FIG. 1. Two experimental I-V curves at 4.2 K taken at the same tip position on a grain of diameter $\sim$8 nm. The tip-sample separation and consequently the value of Q_0, indicated in the figure, were different for the two curves. Curve (a) shows a superconductor gap structure while (b) exhibits Coulomb blockade. The two theoretical curves (smooth lines) were calculated assuming a NINIS tunneling configuration; see text. Curves are shifted for clarity.

A more interesting interplay between SEC effects and superconductivity is manifested in Fig. 2. Here we plot two experimental curves that, again, were acquired at the same lateral position on a surface grain of size $\sim$10 nm, each with a different STM setting. These two curves are part of a set of measurements, all taken with the same bias setting but with different current settings. *All* the traces in this set have shown a pronounced gap structure, but with oscillating width [see Fig. 3(a)]. Here we present only two curves of maximal (a) and minimal (b) gap, both having, in addition, a step at a higher bias voltage. Around the onset of the tunneling current the two curves have a shape which is typical for NIS tunnel junctions. The dynamic conductance dV/dI (not

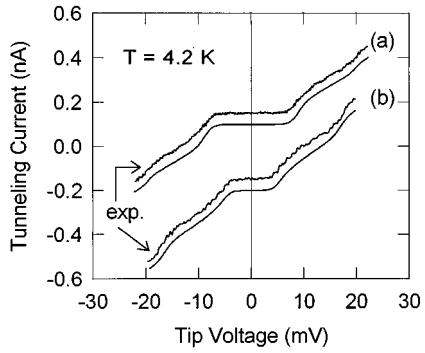

FIG. 2. Two experimental I-V curves at 4.2 K taken at the same lateral tip position on a superconducting grain of diameter ~10 nm, but with *slightly* different tip-sample separations. The curves manifest an interplay between charging effects and superconductivity. The two theoretical curves (smooth lines) were calculated assuming a NISIN configuration as explained in the text. Curves are shifted for clarity.

shown here) indeed manifests the quasiparticle DOS in a superconductor. The minimum apparent gap, however, is about *two times larger* than that observed[10] in the large superconducting regions. We believe that the data obtained at this tip position can be accounted for assuming a DBTJ with a *small superconducting grain* serving as the central electrode (NISIN configuration), as will be discussed below.

In a DBTJ the voltage drop across each junction is only a fraction of the applied voltage, determined by the capacitance of the two junctions. Therefore, when the grain is superconducting and $Q_0=e/2$ (the Coulomb blockade is completely suppressed), the onset of current for zero temperature is at $V_t=(\Delta/e)(C_1+C_2)/C_{\max}$, where $C_{\max}=\max(C_1,C_2)$. At bias voltages just above V_t, the I-V characteristic is dominated by the quasiparticle DOS in the grain, because of the singularity in the DOS near the superconductor gap. At finite temperatures the onset of current is at a smaller voltage, due to the thermal broadening. This scenario is manifested in curve (b) of Fig. 2, with $C_1\approx C_2$. At the other extreme, when $Q_0=0$ (the Coulomb blockade is maximal) the onset of current (for $T=0$) is at $V_t=(\Delta/e)(C_1+C_2)/C_{\max}+e/2C_{\max}$, where $e/2C_{\max}$ is the Coulomb blockade half-width in a normal DBTJ. In this case too, V_t reduces at finite temperatures and the quasiparticle DOS governs the current behavior right above onset. This scenario is depicted in curve (a). At bias voltages well above V_t the quasiparticle DOS in the grain becomes constant (metallic) and thus SEC features, the Coulomb staircase in this case, dominate the I-V curves. This is the origin for the steps observed at $V\approx 20$ mV in curve (a) and at $V\approx 17$ mV in curve (b). The theoretical curves in Fig. 2 were calculated from a model taking into account both the "orthodox" theory for DBTJ and the BCS quasiparticle DOS in the center grain. Both curves were calculated with $C_1=C_2=1.3\times10^{-17}$ F and $\Delta=2.55$ meV, but taking $Q_0=0$ for curve (a) and $Q_0=e/2$ for curve (b). The theoretical curves fit well to the experimental I-V characteristics, and reproduce both the superconducting shape near the onset of tunneling current and the Coulomb steps at higher voltages. One can argue here that, in addition to Q_0, the capacitance C_1, which corresponds to the tip-grain junction, should also be affected by changing the STM setting. A careful look at the experimental details shows, however, that C_1 changes by only a few percent.[10] This change is too small to affect the position of the steps, but large enough to change Q_0 (mod e) by $e/2$, as can be seen from the expression[6,7] $Q_0=(C_1\Delta\Phi_1-C_2\Delta\Phi_2)/e$, where $\Delta\Phi_i$ is the work function difference across junction $i=1,2$.

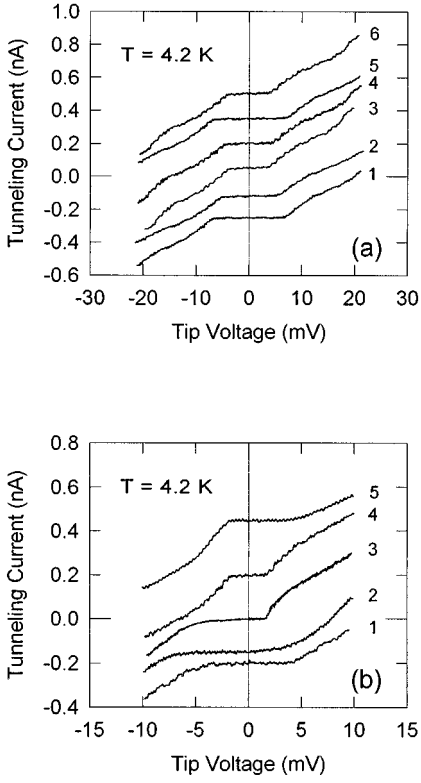

FIG. 3. Two sets of I-V curves, each measured at the same lateral tip position but with different STM setting currents. Set (a) was measured at the same position as in Fig. 2 (NISIN configuration) with $V_s=50$ mV and I_s varying from 0.9 nA (curve 1) to 1.15 nA in increments of ~0.05 nA. Set (b) was measured at the same position as in Fig. 1 (NINIS configuration) with $V_s=35$ mV and I_s increasing from 1 nA (curve 1) to 1.1 nA. Note the difference in the scales of the tip voltage axes.

The difference of the gap-structure evolution between the NINIS configuration and the symmetric ($C_1\approx C_2$) NISIN configuration is clearly manifested by Fig. 3. In Fig. 3(a) we present traces taken at the same tip position as for Fig. 2 (NISIN), all measured with $V_s=50$ mV but with I_s varying from 0.9 nA (curve 1) to 1.15 nA in increments of ~0.05 nA. In Fig. 3(b) we present traces taken at the same tip position as for Fig. 1 (NINIS). In this case all the traces were measured with $V_s=35$ mV and I_s was varied from 1 nA (curve 1) to 1.1 nA. Both sets show variations in the gap structure as a function of the current setting. However, the evolution of the gap structure is markedly different between the two sets. In set (a), which we attribute to the symmetric NISIN geometry, all the I-V curves are relatively symmetric with respect to zero bias. The onset of current always occurs at V_t which is at least twice as large as that observed[10] for the NIS tunnel junction. The shapes of the I-V curves right after the onset of current are all consistent with a superconductor DOS, in our

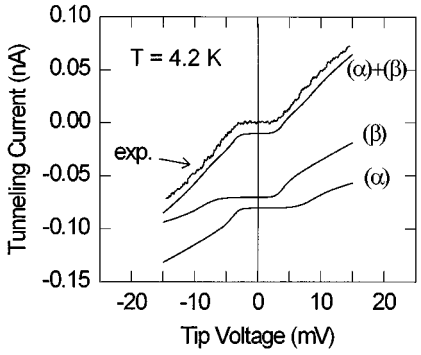

FIG. 4. An I-V characteristic measured on the same grain as in Fig. 2, after making a *large* change in the tip-sample separation. The two theoretical curves (α) and (β) represent the currents carried by the corresponding channels shown in Fig. 5, as explained in the text. The upper theoretical curve represents the total current. Curves are shifted for clarity.

case, that of the small superconducting central electrode. The fluctuation of the gap width is due to the oscillations of Q_0 (mod e), namely, to the variation of the charging energy involved in the tunneling process. The charging energy is minimal for curves 3 and 6, and maximal for 1 and 5. (The behavior of the asymmetric NISIN configuration is more complicated, and will be discussed in the following paragraphs.) Set (b), which we attribute to an asymmetric NINIS geometry, exhibits a more complex behavior. Here the Coulomb blockade, and consequently the I-V characteristics, are not symmetric with respect to zero bias, except for the special cases of $Q_0=0$ or $e/2$ discussed above and depicted by curves 1 and 4, respectively. In curve 2, where $Q_0\approx 0.25e$, the Coulomb blockade is still large enough to mask the superconductor DOS of the substrate for both positive and negative tip voltages. In curve 3, on the other hand, the threshold voltage for the Coulomb blockade is much smaller than Δ for a positive tip bias, but larger than Δ for negative bias. Consequently, this curve exhibits a structure typical of the NIS tunnel junction configuration for positive bias while showing a Coulomb blockade structure for negative bias. We have found that this curve can be accounted for assuming $Q_0\approx 0.35e$. Curve 5 exhibits exactly the same behavior, but for reversed tip bias; here $Q_0\approx -0.35e$.

We have also measured I-V curves at the same tip position as in Fig. 2 after making *major* changes in C_1, resulting in an asymmetric NISIN geometry. For the case where $C_1 \gg C_2$, we have found that the minimal gap (as a function of I_s) approached the NIS value ($V_t\sim\Delta/e$). This fact rules out the possibility of a NISIS configuration, where V_t cannot get much smaller than $2\Delta/e$.

An experimental I-V characteristic of minimum gap ($Q_0=e/2$), taken for the same grain as above, after making a *major* change in the setting is shown in Fig. 4. Here we used $V_s=20$ mV and I_s, $\sim$0.1 nA. Surprisingly, in contrast to the minimal-gap curve in Fig. 2 (where $C_1=C_2$), it appears as if this curve does not simply reflect the quasiparticle DOS in the grain. A closer examination of the NISIN configuration indeed shows that the description given in the previous paragraph is not complete. Due to the gap in the quasiparticle DOS around the Fermi level of the grain, E_F, there are two conduction channels which largely contribute to the total tunneling current through this DBTJ. One is for electrons with energy above $E_F+\Delta$ and the other for electrons with energy below $E_F-\Delta$ (adopting the ''semiconductor model''[13]). The two channels are denoted as channel α and β, respectively, in Fig. 5(b). At $T=0$, the tunneling process in channel α is initiated by an electron that hops *onto* the grain; this occurs through the left junction, junction 2 in Fig. 5, for the bias polarity shown in this figure. Exactly the opposite holds for channel β, where quasiparticles first tunnel *off* the grain through junction 1 (for the same bias polarity). Each channel will open for tunneling when the voltage drop across the corresponding ''initial'' junction will exceed Δ/e. The first will open at $V=\pm(\Delta/e)(C_1+C_2)/C_{\max}$ while the second will start conducting at $V=\pm(\Delta/e)(C_1+C_2)/C_{\min}$ where $C_{\min}=\min(C_1,C_2)$. In Fig. 5 we depict the situation where $C_2>C_1$, where, for the bias polarity shown, the current is onset at channel β first [Fig. 5(a)] and only at a higher voltage current starts flowing through α [Fig. 5(b)]. At the reversed bias the onset voltages are interchanged between the two channels, and channel α will be opened first.

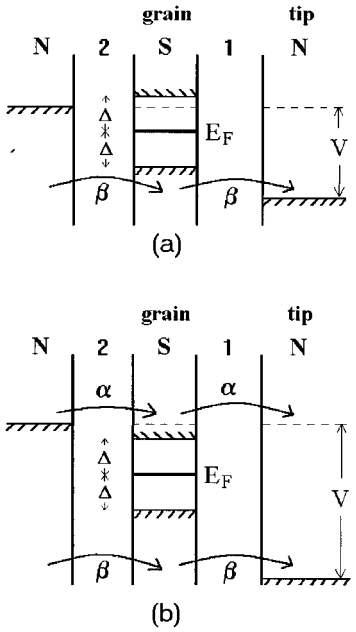

FIG. 5. A schematic ''semiconductor model'' energy diagram of the NISIN tunneling configuration for $C_2>C_1$ and $Q_0=0$. The two possible conduction channels are indicated in the figure. For the bias polarity shown, channel (β) is opened for tunneling first (a), and only at a larger bias voltage channel (α) starts conducting (b).

When $C_1=C_2$ the two channels open simultaneously, independent of the value of Q_0, and contribute identically to the total tunneling current. The superconductor DOS will thus be clearly manifested by the I-V curves, as in the simple NIS configuration. This situation is demonstrated by curve (b) in Fig. 2 and in Fig. 3(a). On the other hand, when $C_1\neq C_2$ the channels open for tunneling at different voltages, even for $Q_0=e/2$. The onset of current through the second channel yields an additional weak step in the I-V characteristic and, more importantly, interferes with the superconductor gap structure manifested by the first channel. This scenario is depicted by the experimental I-V curve in Fig. 4, which indeed does not at all conform to the NIS tunnel junction. In this figure we plot also three theoretical curves. The

two curves labeled (α) and (β) represent the currents carried by the corresponding *single* channels, and were calculated from the BCS theory taking into account the voltage division across the junctions. Note that the I-V curves of the single channels are asymmetric with respect to zero bias. The fitting parameters are $\Delta=2.55$ meV, $C_1=0.95\times10^{-17}$ F, and $C_2=1.3\times10^{-17}$ F, yielding the ratios $(C_1+C_2)/C_1\approx1.73$ and $(C_1+C_2)/C_2\approx2.36$. The sum of the two single-channel contributions is represented by the upper theoretical curve (displaced for clarity from the experimental characteristic), which accounts well for our experimental data.

In summary, we have presented a cryogenic STM study of YNi_2B_2C samples which constitute a disordered granular superconducting-normal system. The simultaneous topography and tunneling-spectroscopy measurements have demonstrated a correlation between the surface morphology and the electronic properties. Spatial transitions from superconducting regions, having a gap parameter $\Delta\cong2.55$ meV, to normal regions occur over distances of $\sim$20 nm. These sharp transitions always take place across grain boundaries, suggesting a weak coupling (large contact resistance) between the grains. The granularity of our samples is clearly manifested by tunneling I-V characteristics which display charging effects, frequently in parallel with superconductivity. Various types of characteristics have been observed, corresponding to different configurations of normal-superconductor DBTJ. The NISIN configuration, in particular, have shown interesting features due to the presence of two tunneling-conduction channels acting in parallel. The effect of the interplay between these two channels on the I-V curves strongly depends on the degree of asymmetry of the tunneling junctions. The flexibility provided by the STM to continuously change this degree of asymmetry, in contrast to the case of nanofabricated structures, enabled us to shed light on the NISIN configuration. Our theoretical I-V characteristics calculated for the different configurations account well for the experimental data.

This work has been supported by the Israel Science Foundation Grant No. 032-7625.

*To whom correspondence should be addressed.

[1] B. Abeles, Phys. Rev. B **15**, 2828 (1977).
[2] L. J. Geerlings, M. Peters, L. E. M. de Groot, A. Vebruggen, and J. E. Mooij, Phys. Rev. Lett. **63**, 326 (1989).
[3] T. E. Eiles, J. M. Martinis, and M. H. Devoret, Phys. Rev. Lett. **70**, 1862 (1993).
[4] M. T. Touminen, J. M. Hergenrother, T. S. Tighe, and M. Tinkham, Phys. Rev. Lett. **69**, 1997 (1992).
[5] *Single Charge Tunneling; Coulomb Blockade Phenomena in Nanostructures*, edited by H. Grabert and M. H. Devoret (Plenum, New York, 1992).
[6] A. E. Hanna and M. Tinkham, Phys. Rev. B **43**, 5919 (1991).
[7] Z. Y. Rong, A. Chang, L. F. Cohen, and E. L. Wolf, IEEE Trans. Magn. **28**, 67 (1992).
[8] W. Wu and P. W. Adams, Phys. Rev. Lett. **73**, 1412 (1994).
[9] E. Bar-Sadeh, Y. Goldstein, C. Zhang, H. Deng, B. Abeles, and O. Millo, Phys. Rev. B **50**, 8961 (1994); E. Bar-Sadeh, Y. Goldstein, M. Wolovelsky, D. Porath, C. Zhang, H. Deng, B. Abeles, and O. Millo, J. Vac. Sci. Technol. B **13**, 1084 (1995).
[10] E. Bar-Sadeh, I. Felner, U. Asaf, and O. Millo, Phys. Rev. B **52**, 6734 (1995).
[11] K. A. McGreer, J. C. Wan, N. Anand, and A. M. Goldman, Phys. Rev. B **39**, 12 260 (1989).
[12] R. J. Cava, H. Takagi, H. W. Zandbergen, J. J. Krajewski, W. F. Peck, Jr., T. Siegrist, B. Batlogg, R. B. Van Dover, R. J. Fedler, K. Mizuhashi, J. O. Lee, H. Eisaki, and S. Uchida, Nature **367**, 252 (1994).
[13] E. L. Wolf, *Principles of Electron Tunneling Spectroscopy* (Oxford University Press, Oxford, 1989).